TECHNICAL POINT OF VIEW

Guidelines for Standardization of Myocardial Perfusion SPECT Imaging 1.0

Standardization Promotion Subcommittee of the Japanese Society of Nuclear Medicine Technology (JSNMT)

Heart Verification Team Members

Taku Aoki[1], Kotatsu Tsuboi[2] and Kazutaka Miki[3]

Members

Taku Aoki[1], Kenichi Takenaka[4], Hiroyuki Tsushima[5], Akio Nagaki[6], Keiichi Matsumoto[7], Kenta Miwa[8], Kazuaki Mori[9] and Takashi Yamanaga[10]

Chairman of the Standardization Promotion Subcommittee

Masahisa Onoguchi[11]

This manuscript was previously published in The Japanese Journal of Nuclear Medicine Technology in Japanese [Aoki T, Tsuboi K, Miki K et al. 心筋血流SPECT撮像の標準化に関するガイドライン1.0. The Japanese Journal of Nuclear Medicine Technology 2020; 40: 413–26. http://plaza.umin.ac.jp/jsnmt/wp-content/uploads/2021/08/d6fec03545ae9449fe53aa27f97b017a.pdf]. This manuscript is an English translated version with permission of JSNMT.

Ann Nucl Cardiol 2022; 8 (1): 91–102

Table of Contents

1. Introduction

Myocardial perfusion single-photon emission computed tomography (SPECT) is used to detect stenotic lesions in ischemic heart disease and to evaluate its severity, prognosis, and myocardial viability (1–5). High class of evidence has been shown in national guidelines (6). However, myocardial perfusion SPECT images are output differently in each institution because many factors such as acquisition, processing, and display conditions affect the image quality (7).

doi: 10.17996/anc.22-004

1) Kariya Toyota General Hospital, Aichi, Japan
2) Hamamatsu Red Cross Hospital, Shizuoka, Japan
3) Asahi University Hospital, Gifu, Japan
4) Izumi Municipal Izumi Clinic, Osaka, Japan
5) Ibaraki Prefectural University of Health Sciences, Ibaraki, Japan
6) Kurashiki Central Hospital, Okayama, Japan
7) Kyoto College of Medical Science, Kyoto, Japan
8) International University of Health and Welfare, Tochigi, Japan
9) Toranomon Hospital, Tokyo, Japan
10) Osaka Metropolitan University Hospital, Osaka, Japan
11) Kanazawa University, Ishikawa, Japan

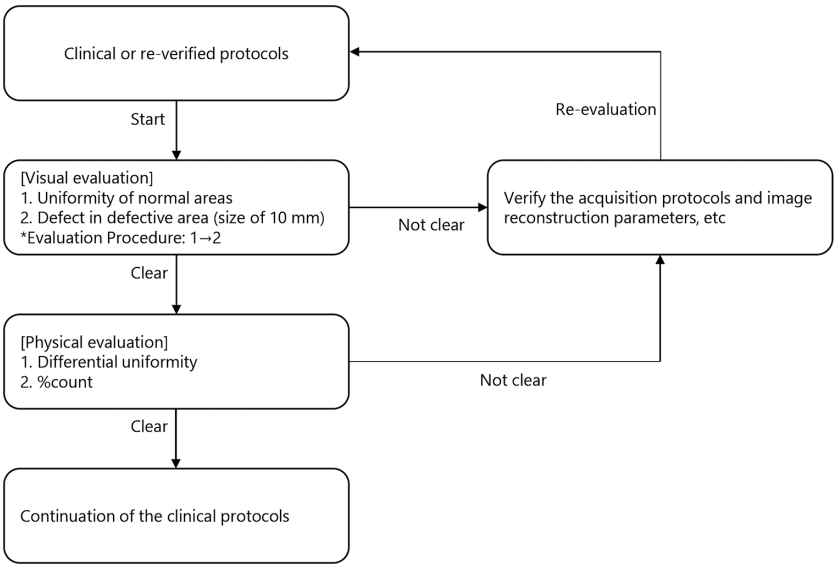

Figure 1 Flow of Verification under this Guideline.

In September 2002, a working group of the Japanese Society of Nuclear Medicine Technology (JSNMT) established to study the quantification and standardization of nuclear medicine images confirmed that many acquisition and processing conditions are determined based on the recommendations of equipment manufacturers and inheritance of past conditions (7).

In 2008, the Working Group for Quantification and Standardization of Images (Points for acquisition processing, display, and output of clinically useful reference images) of the JSNMT published a guideline that proposed specific acquisition and image reconstruction conditions and display methods for reference images of myocardial perfusion SPECT (8). However, there is still a search for standardization, and the reality is that each region is conducting this work independently (9). The reasons for this include the absence of a standard image, the inability to determine the level of images at one's own institution, and image bias among physicians. Therefore, we have developed a guideline to serve as a standard for the use of a standardized phantom, and hereby publish the guideline.

2. Concept of standardization in the cardiac field

Compared to the aforementioned 2008 working group report, various technologies are currently being researched and developed to improve the diagnostic accuracy of myocardial perfusion SPECT images, and are being used in clinical practice (10–12). Therefore, it is difficult to describe uniform acquisition and processing conditions in the guideline. In this guideline, the evaluation system of myocardial image based on technical grounds (EMIT) phantom (Patent No. 5198023, registered on February 15, 2013) (13), which has a simple structure, is used to create and display short-axis images under the acquisition processing conditions used in clinical practice. We propose a method of standardization (Figure 1) by creating and displaying short-axis images under the acquisition and processing conditions used in clinical practice and by clearing the bottom line. The target systems are two-detector and three-detector Anger-type SPECT systems (including diagnostic CT-equipped SPECT systems), and the type of collimator used and the type of image reconstruction are not specified.

For the bottom line, we used 17 data of myocardial SPECT with EMIT phantoms, mainly from facilities of the Tokai Regional Meeting of the JSNMT. The bottom line presented is for the ^{99m}Tc tracers.

3. Phantom

The EMIT phantom to be used is shown in Figure 2 and 3. The structure of this phantom consists of an outer container that imitates the chest and an inner container corresponding to the myocardial part. The myocardial part is used for spatial resolution measurement (defect size) with four defect sizes of 5, 10, 15, and 20 mm and a fixed defect thickness of 10 mm, and for contrast resolution measurement (defect thickness with four defect thickness of 2.5, 5, 7.5, and 10 mm and a fixed defect size of 20 mm. The eight simulated defects are evenly arranged on the contralateral side. Not only can the eight defects be evaluated simultaneously in a single acquisition, but the defects can be positioned freely in the myocardial area: anterior wall, septum, inferior wall, and lateral wall.

4. Phantom creation and analysis methods

4.1 Phantom preparation

In clinical practice, ^{99m}Tc-labeled myocardial perfusion tracers are generally administered at doses of 555 to 1,110 MBq (6), of which the accumulation rate in the myocardium is

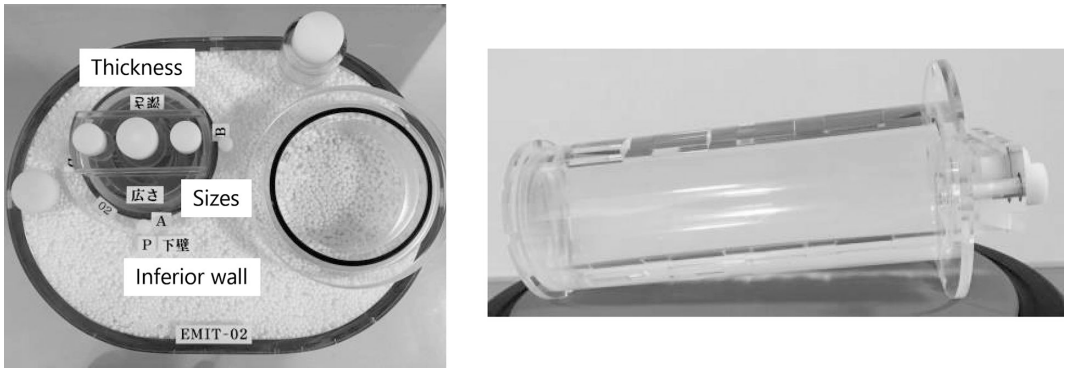

Figure 2 Appearance of the EMIT phantom.

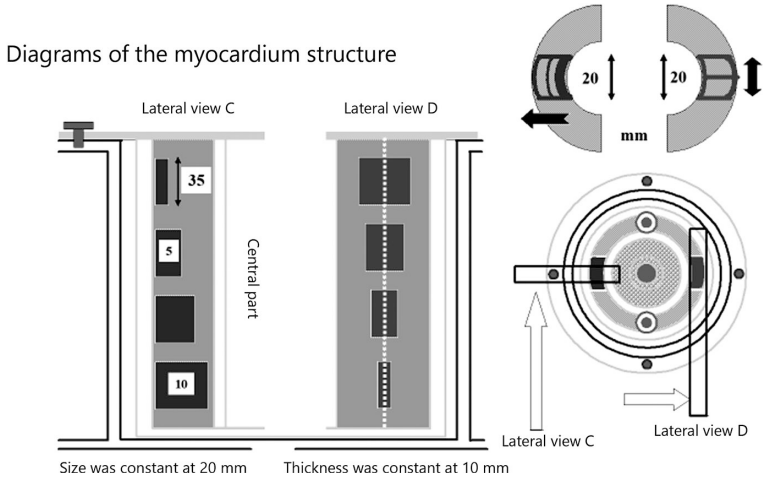

Figure 3 Overview of the inner container of the EMIT phantom.

Table 1 ^{99m}Tc radioactivity per 400mL

Adjustment time	Radio activity
2 hours before	23 MBq – 28 MBq
1 hour and 45 minutes before	22 MBq – 27 MBq
1 hour and 30 minutes before	21 MBq – 26 MBq
1 hour and 15 minutes before	21 MBq – 25 MBq
1 hour before	20 MBq – 25 MBq
45 minutes before	20 MBq – 24 MBq
30 minutes before	19 MBq – 23 MBq
15 minutes before	19 MBq – 23 MBq
At the start of acquisition	**18 MBq – 22 MBq**

reported to be less than 2% (14). The myocardial portion of the EMIT phantom is 375 mL. Therefore, the radioactivity concentration (^{99m}Tc) to be contained in the myocardial part was set at 50 kBq/mL. First, the lumen of the inner container (volume: approximately 265 mL) is filled with water using a funnel provided with the phantom. Four hundred mL of distilled water is prepared, and an appropriate amount of radioactivity is added to the water to reach 18 to 22 MBq at the start of acquisition, referring to Table 1 below, and the water is thoroughly stirred. This radioactivity level of ^{99m}Tc is important and must be observed.

Inject the ^{99m}Tc solution into the myocardium part (Figure 4). Remove the two screws of the spout, close the side (B) without the air vent when about 80% of the solution is injected, and guide air bubbles into the air reservoir (D).

The inner container is installed so that the defect sizes (5, 10, 15, and 20 mm) for spatial resolution measurement are on the inferior wall (the air reservoir is on the lateral wall), and the inner container is fixed so that A of the inner container is aligned with P on the outer phantom container (Figure 5).

4.2. Imaging method

The EMIT phantom is placed horizontally to the bed using a level (Figure 6), and the acquisition is performed under the usual clinical conditions. The EMIT phantom is a static phantom. In facilities where ECG gated acquisition is performed under clinical conditions, acquisition should be performed using a simulated ECG generator, or SPECT acquisition should be performed using non-ECG gated acquisition.

4.3. Image reconstruction methods

The data used in the evaluation of this guideline are non-ECG gated or ECG gated data-summed images. Short axis images are obtained under the image reconstruction conditions

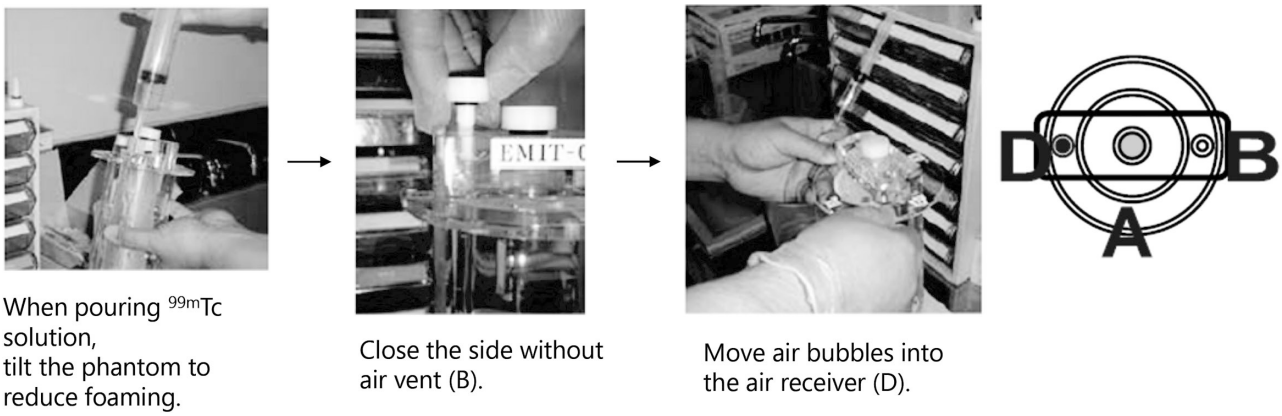

Figure 4　Precautions when injecting ^{99m}Tc solution.

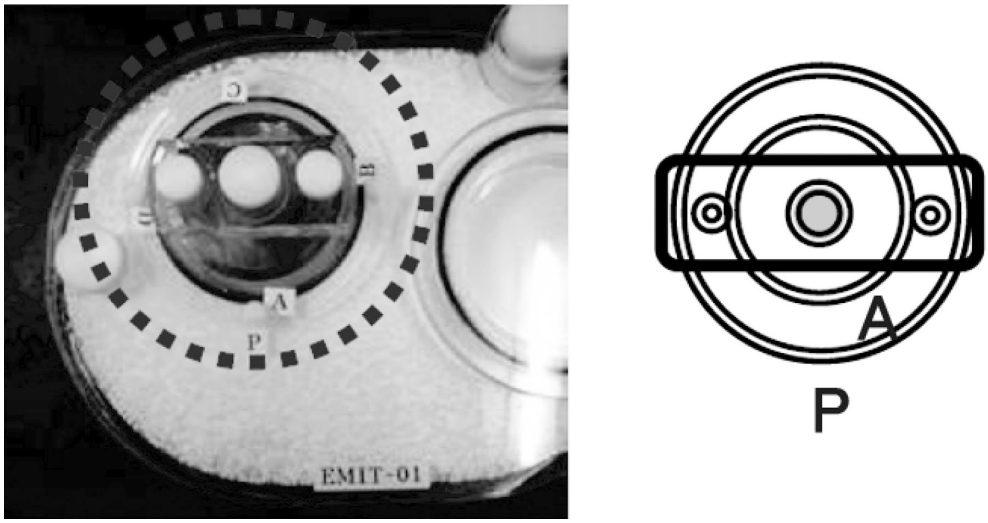

Figure 5　Direction of installation of inner container.

Figure 6　Layout of the EMIT phantom.

used in normal clinical practice, with the air reservoir on the side of the lateral wall. At this time, a wide range is set so that the air reservoir of the EMIT phantom is included in the image reconstruction area (Figure 7).

4.4. Analysis method

Analysis is performed using analysis software dedicated to the EMIT phantom (Figure 8).

The software automatically aligns the SPECT image with the template image of the CT image, and uses the air reservoir as a landmark, so that the image cannot be displayed if it is not included. Then, the development of the aligned image is subjected to circumferential profile analysis (Figure 9) to create the development.

Three hundred and sixty radial lines of 1° each are drawn from the center of each cross-section, and the maximum counts on the lines are plotted. The development fiewis created by expressing the number of slices on the vertical axis and the % counts of 360 lines on the horizontal axis by color.

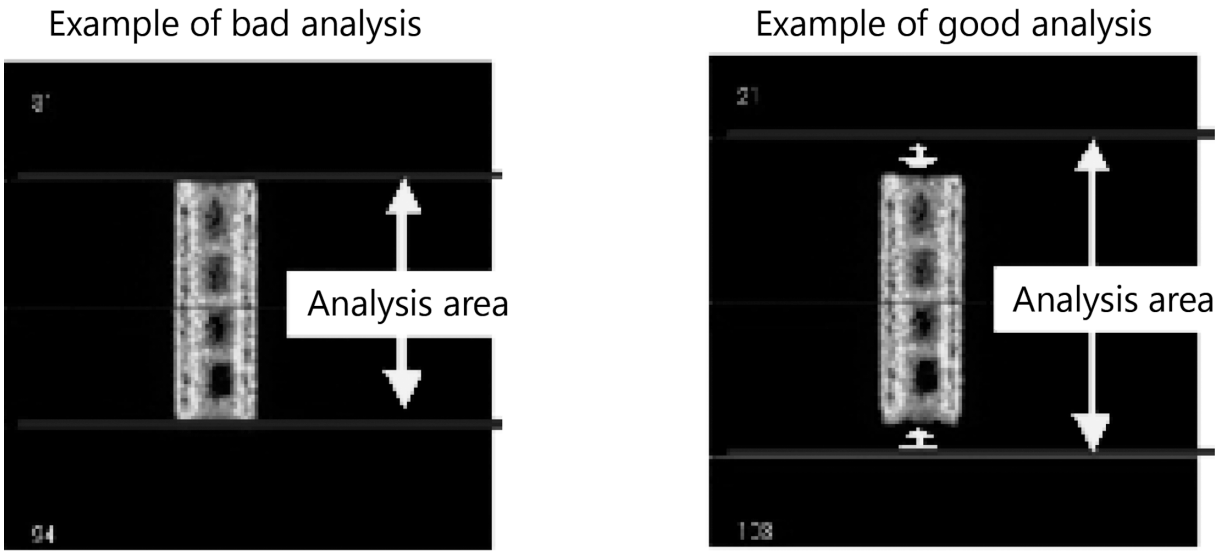

Figure 7 Note on image reconstruction area.

Then, from this development, profile curves in the depth and breadth directions are created as shown in Figure 10 and 11.

Regression lines were drawn connecting the minimum points of each of the obtained profile curves, and the slopes and intercepts were obtained. By automatically evaluating the thickness and size of the defect, each of the indices described below is calculated (Figure 12).

5. Image evaluation

In myocardial perfusion SPECT studies, it is important to be able to point out ischemia or infarction in the myocardium as hypoperfusion areas or defects. Considering the detection limit of SPECT (15), visual and physical evaluation was performed using slices in which 10 mm in defect extent was depicted on the inferior wall.

5.1 Visual evaluation

For visual evaluation, use the reading monitor used at each institution. The monitor displays the slice with the widest 10mm defect in the inferior wall. Evaluation is performed by a physician who reads myocardial perfusion SPECT images at each institution or a radiological technologist in charge of nuclear medicine examinations (board certified nuclear medicine technologist).

First, the normal area without defects in the septum and lateral wall (normal area) is evaluated in five levels of uniformity with reference to the index image for uniformity evaluation shown in Figure 13.

5. Sufficient uniformity is ensured.

4. A slight difference in density in the normal area.

3. A slight difference in density in the normal area and irregularity in the myocardial limbus.

2. Uniformity is conspicuous and moderate image distortion is observed.

1. overall heterogeneity and severe image distortion

Next, for a defect of 10 mm in the inferior wall, the defect delineation ability is evaluated in 5 levels, referring to the index image for defect evaluation shown in Figure 14, and the average score is calculated.

5. Severe reduced accumulation

4. Moderately reduced accumulation

3. Mildly reduced accumulation

2. Equivocal

1. No reduced accumulation

5.2. Physical Evaluation

Physical evaluation is performed using software. The software does not need to be installed on the computer for reading at each facility. The operating system must be Windows, but analysis can be performed by launching the executable file. If SPECT image data can be read, there is no problem even if the software is processed on a stand-alone PC.

5.2.1 Differential uniformity

The maximum deviation (the percentage of the difference between the maximum and minimum values divided by the sum of them) is calculated for every 5 pixels in the region without defects in the septum and lateral wall, and the maximum value in the region is the differential uniformity of each region. The maximum value for the lateral and septum walls shall be calculated as the differential uniformity.

5.2.2. % Count

The percentage of the minimum count value that corresponds to a defect of 10 mm in width placed on the inferior wall divided by the maximum count value of the same slice.

6. Setting the bottom line

6.1. Used EMIT phantom data

The 17 data were imaged using the acquisition and image reconstruction conditions used in clinical practice. The acquisition and image processing conditions at each institution

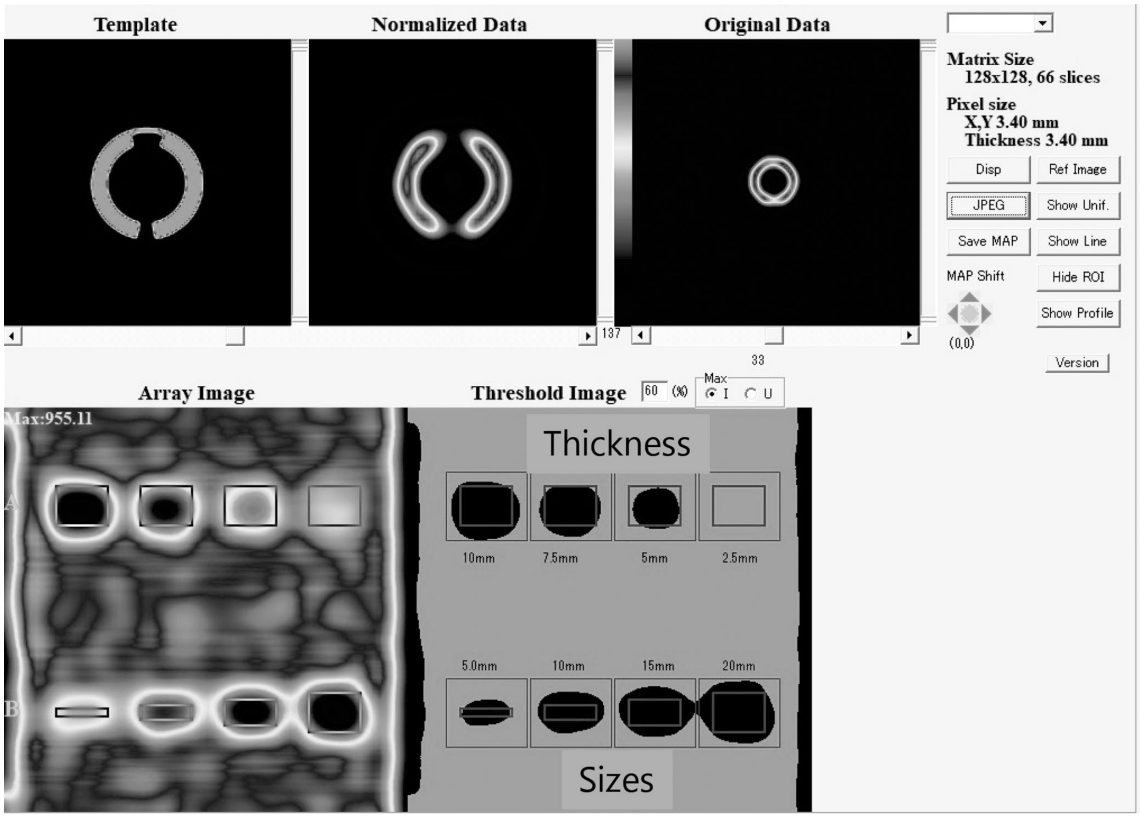

Figure 8 Software screen.

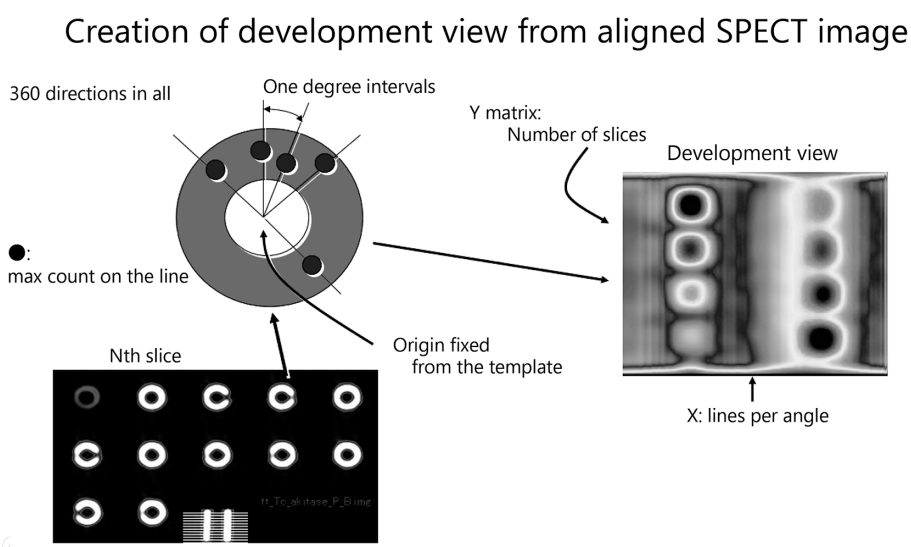

Figure 9 Circumferential profile analysis.

are included in the Appendix (Table 4) at the end of this report. Pixel size ranged from 4.8 mm to 7.8 mm, acquisition time ranged from 20 to 60 sec/step, 9 data were acquired at 360 degrees, and 8 data were acquired at 180 degrees. The image reconstruction method was the filtered back projection method (FBP) with no attenuation, scatter, or resolution correction.

6.2. Setting the bottom line

The bottom line was calculated based on visual evaluation because of the different acquisition and processing conditions at each facility. Visual evaluation was performed by members of the guideline development expert team. The results are shown in Table 5 (Appendix). The mean values for all data were 3.71 ± 0.59 for the uniformity evaluation and 3.76 ± 0.56 for the defect area evaluation. A uniformity rating of 3 was defined as a slight concentration difference in the normal area and irregular myocardial limbus (edge), whereas here uniformity was maintained. Defect evaluation of 3 was recognized as a 10 mm defect, since it showed a mild decrease in accumulation. In general, the contrast between uniformity

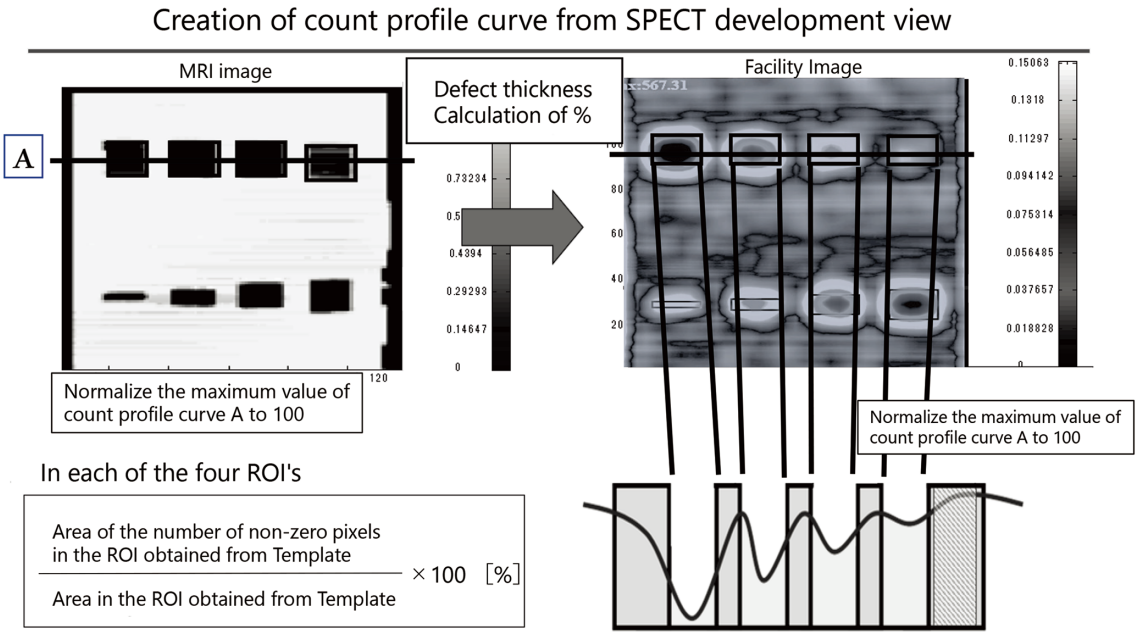

Figure 10 Profile curves in the depth direction of the defect.

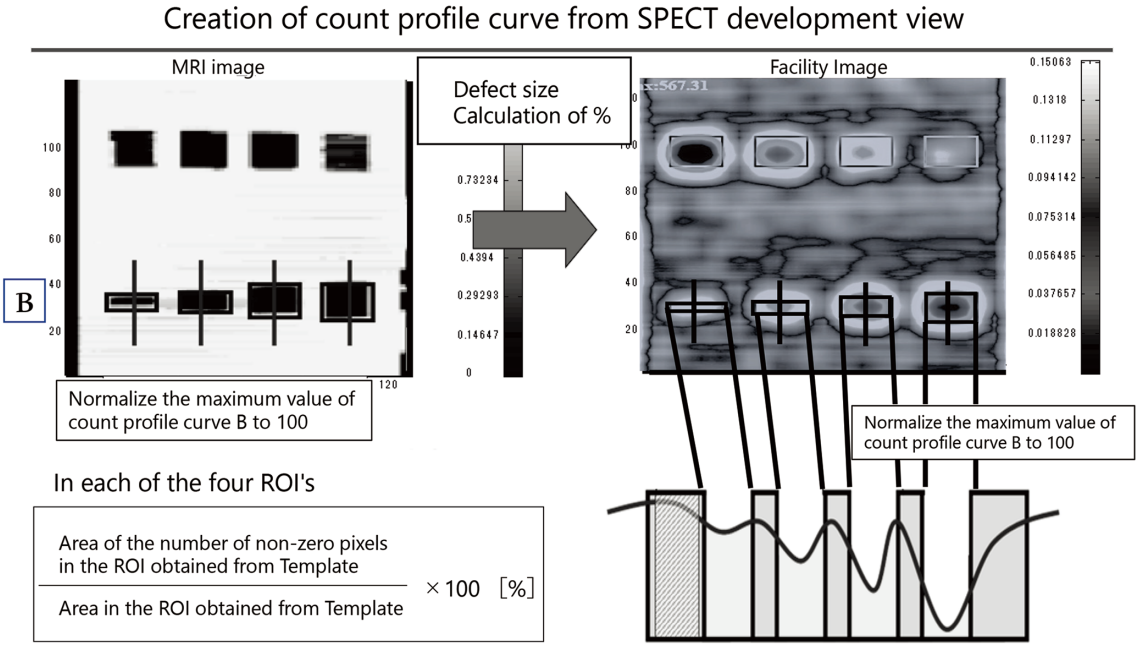

Figure 11 Profile curves in the direction of defect extent.

and defects is an important indicator in visual evaluation. As shown in Figure 1, the first step is to evaluate the uniformity, so if it is not clear whether the defect is a defect or poor uniformity, the uniformity evaluation is not 3, but 2 or 1. Therefore, the bottom line for visual evaluation was defined as 3 or higher for both uniformity and defect evaluation. The bottom line of the physical index was obtained using the data with a visual evaluation of 3 or higher. These visual evaluations and acquisition and processing conditions are listed in the Appendix.

The scores for differential uniformity and % count were 2.60 ± 0.62 and 58.65 ± 7.79, respectively. The bottom line was defined as mean + 2SD for differential uniformity and mean + 1. 5SD for % counts due to the large standard deviation. Table 2 shows the scores. The number of data used to calculate the bottom line of the physical evaluation set this time was n=17, which is presumably small from a statistical point of view. It is desirable to consider increasing the number of data in the future. The FBP method was used as the only image reconstruction method in this study, but data with resolution correction by the OSEM (ordered subset expectation maximization method) and other methods will be discussed in a future issue.

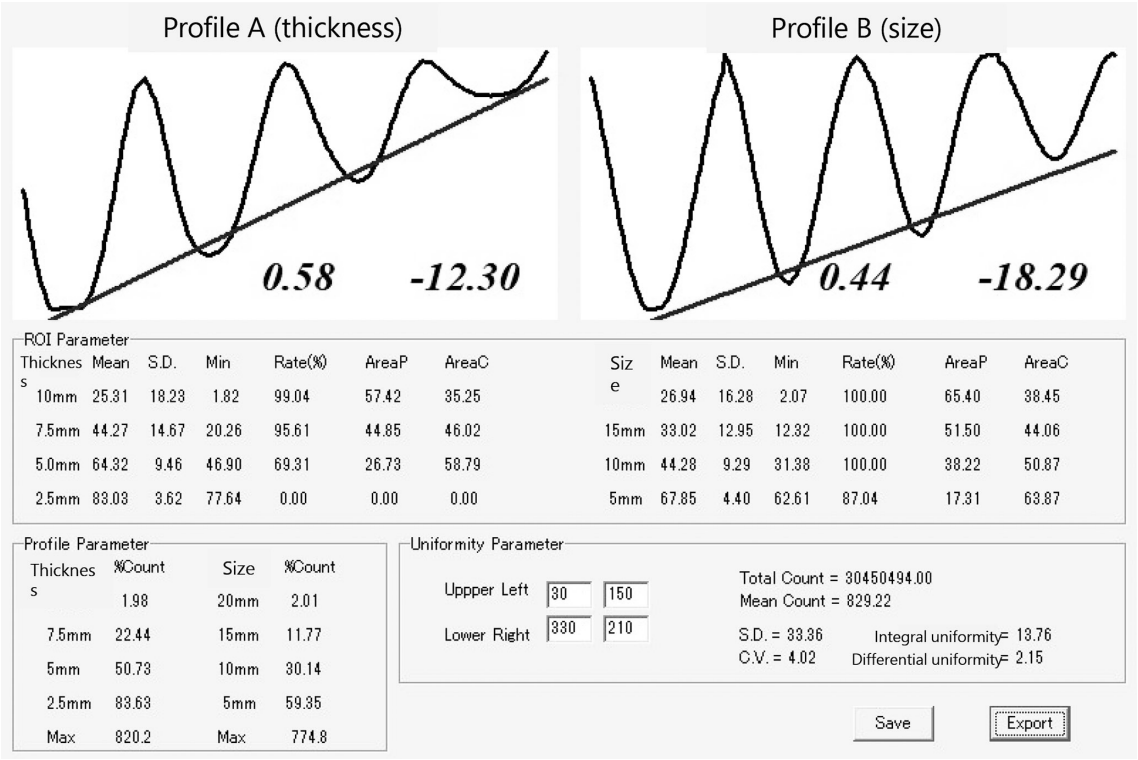

Figure 12 Analysis results for each indicator.

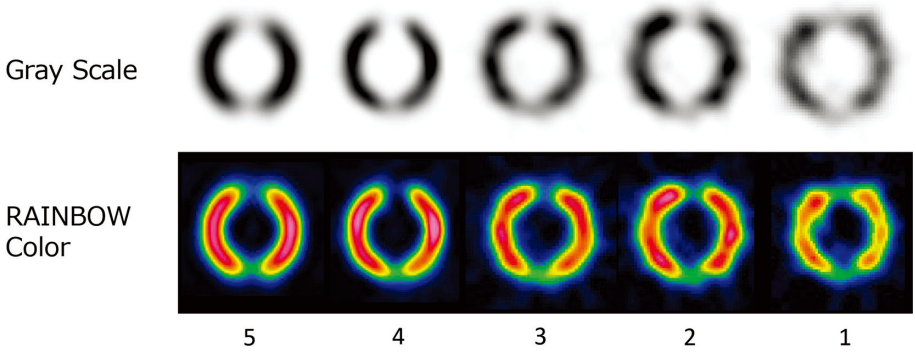

Figure 13 Index image for uniformity evaluation.

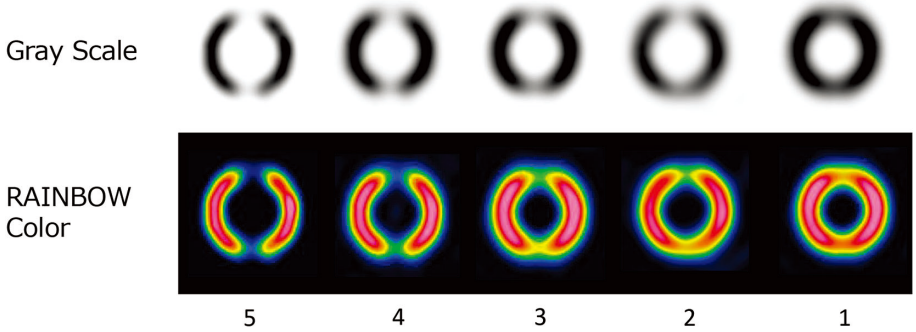

Figure 14 Indicative images for defect evaluation.

Table 2 Bottom line on physical evaluation

	Bottom line
Differential uniformity	≦ 3.84
%count	≦ 70.34

7. Image improvement methods

A flowchart of measures to be taken when the bottom line is not met is shown in Figure 15, and Table 3 shows an example of the acquisition, processing, and display of the ^{99m}Tc-labeled myocardial perfusion SPECT reference images provided in the

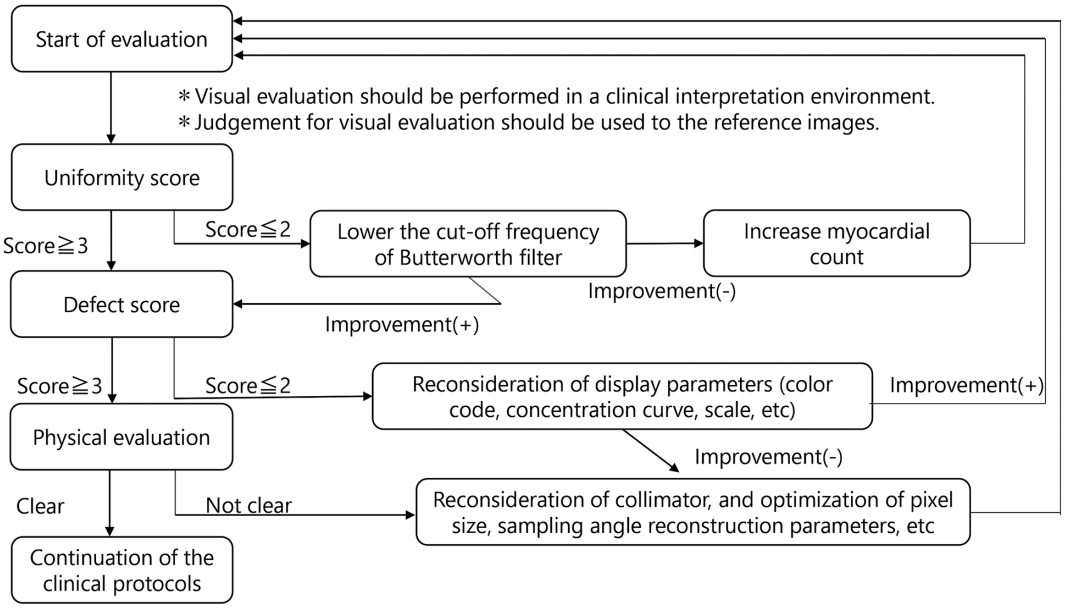

Figure 15 Flowchart when bottom line is not qualified.

Table 3 An example of the collection, processing, and display of ^{99m}Tc agent myocardial blood flow SPECT reference image as presented in the previous guideline

Radiopharmaceuticals	^{99m}Tc-MIBI / ^{99m}Tc-tetrofosmin
Scan conditions	
Collimator	LEHR
Energy window	140 keV ± 10%
Doses	296 - 740 MBq
Sampling angle	5 - 6°
Scan time / step	20-40 sec
Matrix	64 × 64
Pixel size	5 - 7 mm
Reconstruction parameters	
Preprocess filter	Butterworth [order: 5, cut-off: 0.42 cycles/cm]
Reconstruction filter	ramp
Attenuation correction	(-)
Scatter correction	(-)
Display parameter (gray)	
Concentration curve	Square
Display scale	10 - 100%

previous guideline (8). If the bottom line cannot be met in visual evaluation, the method of displaying the images should first be reviewed. Consider changing the color code for color scale, or changing the grayscale to square (lower convex squared curve) or sigmoidal (S-curve) for grayscale. In addition, we also consider increasing the lower level (10–20%) to the extent that the right ventricle and background do not disappear in the clinical image (8). If the bottom line cannot be met even after these measures, it is assumed that many cases do not meet the bottom line in the physical evaluation as well, so we will proceed to measures to improve the physical evaluation first.

If the bottom line could not be met in the physical evaluation, the following points should be reviewed in the acquisition conditions: collimator, acquisition time, pixel size (matrix size and magnification ratio), and number of sampling directions. Reconstruction conditions include processing filters and reconstruction parameters (8). The number of counts per myocardium pixel in the projection data has a significant impact on image quality, so it is necessary to set an appropriate acquisition time. If the number of counts is N, the statistical error (%) can be expressed as $\sqrt{N}/N \times 100$ and the

statistical noise as $\sqrt{N}$. Therefore, the statistical error increases rapidly when the number of counts per pixel falls below 40 to 50. Therefore, an acquisition time of 100 counts or more per myocardial pixel is desirable, which results in a statistical error of 10% or less (16). In general, most facilities perform myocardial perfusion SPECT examinations with both upper limbs, and a single examination time of 20 to 30 minutes or less is appropriate. In facilities where acquisition counts are low and it is difficult to extend acquisition time, changing from a low-energy high-resolution collimator (LEHR) to a low-energy general-purpose collimator (LEGP) or changing the acquisition magnification rate (pixel size) and matrix size (from 128 × 128 to 64 × 64) should be considered. The number of sampling directions suitable for the pixel size can be obtained from the sampling theorem: $N= \pi D/2P$ (14). N is the number of sampling directions, D is the effective field of view (mm), and P is the pixel size (mm). Review the acquisition conditions for the above items, and if there are no problems, review the reconstruction conditions next. When the FBP method is used for image reconstruction, image quality varies greatly depending on the cutoff frequency of the Butterworth filter used as a preprocessing filter (17).

The higher the cutoff frequency, the better the spatial resolution but the noisier the image, and the lower the cutoff frequency, the lower the spatial resolution and the smoother the image. If the bottom line cannot be satisfied with respect to the differential uniformity of the physical evaluation, the cutoff frequency should be set lower. For the % count, if the bottom line cannot be satisfied, the cutoff frequency is set higher. However, the setting should be determined in consultation with the diagnostic physicians, since confirmation by the normalized mean square error (NMSE) method (18) and visual evaluation of the clinical data are important. When the OSEM method is used for image reconstruction, the optimal subset and number of iterations are not constant, depending on the device manufacturer and the presence of various corrections (attenuation correction, scattered ray correction, correction for deterioration of spatial resolution due to collimator aperture, etc.) (19, 20). Therefore, first check the value of the post-processing filter (Gaussian filter, etc.), and refer to the 2008 working group report (8) for the number of subsets and iterations. As with the FBP method, the settings should be determined in consultation with the diagnostic physicians.

Guideline for Standardization of Cardiac Fields 1.0 Evaluation Procedure

*Checked items are ticked in □.

1. Preparation of EMIT phantom

□ Is the amount of radioactivity to be contained appropriate? (see Table 1)

□ Was the phantom placed in such a way that the defect size is on the inferior wall? (see Figure 5)

2. imaging

□ Is the phantom placed with the air reservoir facing the head? (see Figure 6)

□ Is the phantom positioned horizontally to the bed?

3. Image Reconstruction

□ Is the image reconstruction performed under the usual clinical conditions?

□ Is the air reservoir included in the reconstruction area? (see Figure 7)

□ Is the air reservoir on the side of the lateral wall? (regardless of the slice No.)

4. Visual evaluation

□ Was the defect evaluated in a normal reading environment?

□ Is the slice with the widest defect (10mm) shown?

1. Uniformity evaluation of normal area (compare the uniformity of septum and lateral wall with the reference image)

Evaluation of own institution: Uniformity score 5・4・3・2・1 <bottom line: 3 or more>

2. Defect evaluation of 10 mm in defect size (compare the defect of the lower wall with the reference image)

Evaluation of own institution: Defect score 5・4・3・2・1 <bottom line: 3 or more>

5. Physical evaluation

□ Is the one with the smallest slice No. the air reservoir?

□ Is the one with the larger defect on the anterior wall among the defects closest to the air reservoir?

□ Is the air reservoir on the left side in the development view?

Acknowledgments

We would like to thank the people involved in the development of the EMIT phantom and Dr. Tetsuro Katafuchi (Gifu University of Medical Science) for their efforts in publishing this guideline. We would also like to express our gratitude to the patent owner, FUJIFILM RI Pharma Corporation (now FUJIFILM Toyama Chemical Co., Ltd.). We thank Mr. Koichi Fujino (Osaka University Hospital), Chair of the SPECT Standardization Committee of the Japanese Society of Nuclear Medicine and Technology (2014-2018), Dr. Akihiro Kikuchi (Hokkaido University of Science), Mr. Hirotaka Shimada (Gunma University Hospital), Mr. Atsushi Narita (Nihon Medi-Physics Co., Ltd.), and Mr. Kazuaki Mori (Toranomon Hospital) for their guidance from the beginning in preparing these guidelines. Finally, we would like to thank all the institutions that provided us with images.

References

1. Nakajima K, Kusuoka H, Nishimura S, Yamashina A, Nishimura T. Normal limits of ejection fraction and volumes determined by gated SPECT in clinically normal patients without cardiac events: a study based on the J-ACCESS database. Eur J Nucl Med Mol Imaging 2007; 34: 1088–96.
2. Sharir T. Role of regional myocardial dysfunction by gated myocardial perfusion SPECT in the prognostic evaluation of patients with coronary artery disease. J Nucl Cardiol 2005; 12: 5–8.
3. Slomka PJ, Nishina H, Berman DS, Akincioglu C, Abidov A, Friedman JD, et al. Automated quantification of myocardial perfusion SPECT using simplified limits. J Nucl Cardiol 2005; 12: 66–77.
4. Matsumoto N, Sato Y, Suzuki Y, Kasama S, Nakano Y, Kato M, et al. Incremental prognostic value of cardiac function assessed by ECG-gated myocardial perfusion SPECT for the prediction of future acute coronary syndrome. Circ J 2008; 72: 2035–9.
5. Petix NR, Sestini S, Coppola A, Marcucci G, Nassi F, Taiti A, et al. Prognostic value of combined perfusion and function by stress technetium-99m sestamibi gated SPECT myocardial perfusion imaging in patients with suspected or known coronary artery disease. Am J Cardiol 2005; 95: 1351–7.
6. Tamaki N, Kusakabe K, Kumita S, Simamoto K, Senda S, Nishimura T, et al. Guidelines for clinical use of cardiac nuclear medicine (JCS2010). http: //jsnm. org/wp_jsnm/wp-content/themes/theme_jsnm/doc/shinzoukakuigakukensa_gl.pdf
7. Niida H, Ohya N, Katafuchi T, Teraoka S, Yanagisawa M, Saitoh K. Questionnaire report for practical conditions of nuclear medicine examination and standardization of image acquisition, processing, display and output. The Japanese Journal of Nuclear Medicine Technology 2004; 24: 95–118. [Article in Japanese]
8. Masuda Y, Nagaki A, Kawabuchi Y, Ohya N, Katafuchi T, Teraoka S, et al. Point of acquisition, processing, display and output for standardized images with clinical usefulness. The Japanese Journal of Nuclear Medicine Technology 2008; 28: 13–66. [Article in Japanese]
9. Horita H. Details of standardization efforts at the local association level. The Japanese Journal of Nuclear Medicine Technology 2015; 35: 87–90. [Article in Japanese]
10. Van Dijk JD, Jager PL, Ottervanger JP, Slump CH, de Boer J, Oostdijk AHJ, et al. Minimizing patient-specific tracer dose in myocardial perfusion imaging using CZT SPECT. J Nucl Med Technol 2015; 43: 36–40.
11. Armstrong IS, Arumugam P, Lames JM, Tonge CM, Lawson RS. Reduced-count myocardial perfusion SPECT with resolution recovery. J Nucl Med Commun 2012; 33: 121–9.
12. Matsutomo N, Nagaki A, Sasaki M. Performance of myocardial perfusion imaging using multi-focus fan beam collimator with resolution recovery reconstruction in a comparison with conventional SPECT. Asia Oceania J Nucl Med Biol 2014; 2: 111–9.
13. Shibutani T, Onoguchi M, Katafuchi T, Kinuya S. Development of a myocardial phantom and analysis system toward the standardization of myocardial SPECT image across institutions. Ann Nucl Med 2016; 30: 699–707.
14. Nishimura T, Kumita S, TamakiN et al: BRAND NEW Nuclearcardiology- Functional imaging captures pathology 1st editiron, Tokyo, Kanehara & Co., Ltd., 2012. [in Japanese]
15. Nishimura S, Kobayashi H: Nuclearcardiology Complete Manual 1st editiron, Tokyo, 6Medical View Co., Ltd., 2004. [in Japanese]
16. Ogawa K Image quality degradation in SPECT and its correction IV Statistical variation of γ rays A Monthly Journal of Medical Imaging and Information 2002; 34: 1136–40. [Article in Japanese]
17. Ohnishi H, Ushio N, Matsuo S, Takahashi M, Noma K, Masuda K. Optimized Butterworth filters for ^{99m}Tc myocardial perfusion SPECT images: An evaluation. Japanese Journal of Radiological Technology 1996; 52: 346–50. [Article in Japanese]
18. Ichikawa H, Onoguchi M, Tsushima H et al. Radiology and Medical Technology Series (37) ABC book of experiment in nuclear medicine for beginners. 42–55, Public Interest Incorporated Association Japanese Society of Radiological Technology, 2016. [in Japanese]
19. Matsutomo N, Furuya H, Yamao T, Nishiyama N, Suruga T, Sugino S, et al. Comparison of OS-EM reconstruction algorithms among different processors using a digital phantom dedicated for SPECT data evaluation. Japanese Journal of Radiological Technology 2008; 64: 1361–8. [Article in Japanese]
20. Maeda Y, Nagaki A, Komi Y, Abe N, Kashimura S. Evaluation of resolution correction in single photon emission computed tomography reconstruction method using a body phantom: Study of three different models. Japanese Journal of Radiological Technology 2015; 71: 1070–9. [Article in Japanese]

[Appendix]

Table 4 Collection and image reconstruction conditions at each facility

Institution	Scanner	Number of detectors	Collimator	Scan angle	Acquisition matrix	Number of projections	Scan time (sec/step)	Sampling angle (degree)	Pixel size (mm)	Reconstruction method	Reconstruction filter	Preprocess filter	Cut-off frequency (cycles/cm)	Order
A	PRISM-IRIX (SHIMADZU)	3	LEHR	360	64×64	60	20	6	6.3	FBP	Ramp	Butterworth	0.38	8
B	E.CAM (Canon)	2	LMEGP	360	64×64	72	25	5	5.4	FBP	Ramp	Butterworth	0.50	8
C	Symbia E (Canon)	2	LMEGP	360	128×128	60	40	6	4.8	FBP	Ramp	Butterworth	0.42	8
D	PRISM-IRIX (SHIMADZU)	3	LEGP	360	64×64	72	30	5	7.1	FBP	Ramp	Butterworth	0.37	8
E	MillenniumVG (GE)	2	LEHR	180	64×64	30	60	6	6.7	FBP	Ramp	Butterworth	0.45	10
F	E.CAM (SHIEMENS)	2	LEHR	360	64×64	60	30	6	6.6	FBP	Ramp	Butterworth	0.42	10
G	Symbia E (SHIEMENS)	2	LEHR	360	64×64	72	25	5	6.6	FBP	Ramp	Butterworth	0.60	8
H	INFINIA (GE)	2	LEHR	180	64×64	36	45	5	5.9	FBP	Ramp	Butterworth	0.40	10
I	E.CAM (Canon)	2	LEHR	360	64×64	60	40	6	6.6	FBP	Ramp	Butterworth	0.42	8
J	E.CAM (Canon)	2	LEHR	180	64×64	32	40	5.6	5.4	FBP	Ramp	Butterworth	0.42	8
K	PRISM-IRIX (SHIMADZU)	3	LEGP	360	64×64	60	30	6	6.3	FBP	Ramp	Butterworth	0.40	8
L	INFINIA (GE)	2	LEHR	180	64×64	30	40	6	6.8	FBP	Ramp	Butterworth	0.45	10
M	MillenniumVG (GE)	2	LEHR	180	64×64	36	30	5	6.7	FBP	Ramp	Butterworth	0.52	5
N	MillenniumVG (GE)	2	LEHR	180	64×64	30	50	6	5.3	FBP	Ramp	Butterworth	0.54	10
O	E.CAM (Canon)	2	LEHR	180	64×64	60	30	3	7.8	FBP	Ramp	Butterworth	0.45	8
P	E.CAM (Canon)	2	LEHR	360	64×64	60	40	6	6.6	FBP	Ramp	Butterworth	0.42	8
Q	INFINIA (GE)	2	LEHR	180	64×64	30	40	6	6.8	FBP	Ramp	Butterworth	0.45	5

LEHR: low energy high resolution, LMEGP: low-medium energy general purpose, LEGP: low energy general purpose, FBP: filtered back projection

[Appendix]

Table 5 Visual and physical assessment results for each facility

Institution	Visual evaluation		Physical evaluation	
	Uniformity	Defect	Differential uniformity	%count
A	5	4	1.69	47.98
B	4	5	2.52	40.67
C	4	4	2.26	55.77
D	4	4	3.47	59.55
E	4	4	2.24	55.42
F	4	4	2.75	56.72
G	4	4	2.44	52.71
H	4	4	3.72	60.61
I	4	3	2.17	62.09
J	4	3	2.44	70.3
K	4	3	2.25	60.85
L	3	4	2.8	60
M	3	4	3.08	65.31
N	3	4	3.69	50.05
O	3	4	2.69	65.63
P	3	3	1.55	63.56
Q	3	3	2.39	69.91